Journal of King Saud University – Science (2016) **28**, 308–317

King Saud University
Journal of King Saud University – Science
www.ksu.edu.sa
www.sciencedirect.com

ORIGINAL ARTICLE

Combined effect of unsaturated soil condition and soil heterogeneity on methylene blue adsorption/desorption and transport in fixed bed column: Experimental and modeling analysis

Dardouri Sana *, **Sghaier Jalila**

Unité de recherche thermique et thermodynamique de procédés industriels, Ecole national d'ingénieurs Monastir, Monastir 5009, Tunisia

Received 13 October 2015; accepted 18 January 2016
Available online 28 January 2016

KEYWORDS

Methylene blue;
Adsorption/desorption;
Transport;
Unsaturated heterogeneous soil;
Breakthrough curve modeling

Abstract Several series of batch and fixed bed column experiments have been carried out to study the methylene blue sorption and transport in sandy and clay soil under different experimental conditions. The non linear forms of the pseudo-second order kinetic model and the Freundlich and Langmuir isotherm models were used to quantify the maximum adsorption capacity of the used materials. The effects of several experimental factors (flow rate, initial concentration, saturation condition of soil and soil heterogeneity) on the breakthrough curves have been undertaken. Experimental data revealed that the breakthrough curves depend on flow rate, methylene blue inlet concentration, saturation condition of soil and soil heterogeneity. A two dimensional model based on Richards equation and advection–dispersion equation coupled with adsorption model was developed. A comparative analysis between this model and Thomas model showed the effectiveness of advection–dispersion model to describe the experimental breakthrough curves and particularly in an unsaturated heterogeneous medium. The advection dispersion model reproduces perfectly the transfer mechanisms in porous media and seems to be a useful tool to better understanding the physical processes and the effect of capillary barrier of methylene blue transport in unsaturated heterogeneous soil. The result shows also that the soil heterogeneity has a significant effect on methylene blue adsorption through unsaturated layered media. Furthermore, in the interface between two layers with different hydrodynamic proprieties, the adsorption capacity increases with a decrease in kinetic adsorption rate caused by the decrease in pore water velocity.

* Corresponding author.
E-mail addresses: sanadardouri_en@yahoo.fr (D. Sana), jalila.sghaier@enim.rnu.tn (S. Jalila).
Peer review under responsibility of King Saud University.

Production and hosting by Elsevier

http://dx.doi.org/10.1016/j.jksus.2016.01.004

1. Introduction

With the fast development in industrial scale, the problem of water and soil pollution has become more serious. The use of organic dyes in many industrial products may threaten the water systems. For instance, the methylene blue (MB) is a cationic dye which is found in many industrial effluents (textile, cosmetic industries, paper and plastic). It is an important contaminant in soil and water bodies and it may induce health problems (Xing et al., 2010). Hence, the removal of MB is fundamental to ensure the non contaminated water supplies. Several adsorbents were used to remove the MB such as the activated carbons (Yang and Qiu, 2010; Foo and Hameed, 2011), Kapok fiber (Liu et al., 2012), chitosan clay composite (Auta and Hameed, 2014), modified bamboo powders (Guo et al., 2014), Natural zeolite (Wang et al., 2006), sludge (Mitrogiannis et al., 2015), swelling clay (Li et al., 2011), char (Makrigianni et al., 2015) and organo-illite/smectite clay (Wang et al., 2013). The activated carbon is the most used adsorbent for dye removal, but it is costly. As an alternative solution, many low cost adsorbents are examined to replace activated carbons. These adsorbents should be easily available and could be regenerated. Sand is used as an adsorbent in removing dyes (Rauf et al., 2008) and the removal of methylene blue (Bukallah et al., 2007; Dotto et al., 2015). Also, the clay minerals are a good adsorbent with low cost which are still receiving attention because of the various applications in industrial scale due to their attractive adsorption proprieties. The adsorption capacities of these clay minerals for dyes depend on the clay proprieties, the adsorbate and the experimental conditions (Şahin et al., 2015). The sorption to subsurface materials is one of the major processes that dominate the dye transport in soil. This process can be performed using batch and column experiments (Auta and Hameed, 2014; Zhang et al., 2011; Hamdaoui, 2006), but the dynamic adsorption systems (column experiments) are preferred because they describe well the dye adsorption capacity (Reza and Ahmaruzzaman, 2015). Sorption is also one of the most important processes which reduce the chemical infiltration in soils, but it isn't the only dominating process that controls the MB migration in continuous fixed bed column. The MB particles move in the pore space of the medium due to advection by the fluid flow and it is dispersed according to the transport process. Therefore, the mass transfer which occurs along the continuous fixed bed column during MB migration includes three processes: (i) fluid flow, (ii) mass transport and (iii) physical and chemical adsorption. Several experimental factors influence the MB infiltration into the soil. Therefore, the breakthrough curves (BTCs) depend on the fixed bed configuration, flow rate, feed concentration, pH, temperature, adsorbent density, and other variables (Reza and Ahmaruzzaman, 2015). Besides these influencing factors, the soil heterogeneity plays an important role in reducing chemical product infiltration. The presence of capillary barrier influences the transfer of both water and pollutant (Winiarski et al., 2013). The adsorption in the vicinity of the capillary barrier increases and the interface between both porous media became an ideal area for particle detention (Prédélus et al., 2015). In unsaturated medium the transport process is more sophistical than saturated medium due to the presence of air in poral space. This can cause more retention in unsaturated soil (Tian et al., 2011). The high retention capacity in unsaturated soil causes retardation in breakthrough curve profile. The retardation factor increases in soil under dry conditions compared to the porous media under moist conditions (Sadasivam and Reddy, 2015). Indeed, the presence of moisture in soil results in an important decrease in the equilibrium adsorption capacity of soil. Moreover, the increase in moisture content in porous media may also decelerate the transport processes of air phase existing in the pore volume because molecular diffusion in water is slower than in air. The modeling of these breakthrough curves is essential to predict the adsorption behavior using parameters obtained from experimental studies. In fact, several models have been proposed for the correlation of breakthrough curve data obtained in dynamic adsorption process. For example, Thomas model (Thomas, 1944) is one among these several models used to describe the solute adsorption in fixed bed column. It was successfully used for the prediction of breakthrough curves and provides good agreement between experimental and calculated data (Uddin et al., 2009). It has been proved that Thomas model is the most suitable one to describe MB adsorption in column experiment on to modified straw adsorbent (Zhang et al., 2011), Leaf powder (Han et al., 2009), jackfruit leaf powder (Uddin et al., 2009) and natural zeolite (Han et al., 2007). However to model the transport in column adsorption, the advection dispersion model was chosen (Sadasivam and Reddy, 2015) to fit the experimental breakthrough curves obtained under different moisture conditions. In this work, a comparative numerical analysis of two models for breakthrough curves modeling has been studied using experimental data. To model the MB transfer in porous media, it is prerequisite to know the hydrodynamics and solute transport parameters. These parameters have been determined by characterizing the porous media used in this study. The advantage of the advection–dispersion compared to the Thomas model is that the different physical processes can be coupled and solved simultaneously. Furthermore, this model coupled with Richard equation and adsorption kinetic equation can be applied to a variety of materials and takes into account the porous media characteristics, the hydrodynamics and the solute proprieties. Another advantage of this model is the capabilities to study the desorption experiments and to evaluate the adsorbed concentration in solid phase.

The main goal of this study is (i) to study the adsorption–desorption and transport behavior of MB in two soils with different properties (sand and clay) using batch and column experiments; and (ii) to test the capabilities of both models to simulate non equilibrium sorption and transport of MB in soils under different experimental conditions.

2. Materials and methods

2.1. Soil and solutions

Both samples (sand and clay) used in this study were collected from an industrial zone in the region of Sousse in Tunisia. The particle size distribution of sand and clay and the exchange capacity (CEC) of clay were measured by laser diffraction particle size analyzer (Microtrac S3500) and by the Metson method (AFNOR NF X31-130), respectively. The mineralogy of the sand and clay samples was established by X-ray

diffractometer (XPert PRO PANalytical). The reactive dye methylene blue used as adsorbate (basic blue 9, CI 52015) is a cationic dye with a molecular formula $C_{16}H_{18}ClN_3S{\cdot}3H_2O$ and a molar mass of 373.9 $gmol^{-1}$. The wavelength of maximum absorbance for MB is 663 nm (see Table 1).

2.2. Batch experiment

Adsorption isotherms and adsorption kinetics experiments were performed to evaluate the adsorption capacity of MB in two materials.

2.2.1. Sorption isotherms

The adsorption isotherms were performed in a set of glass flasks (60 ml) containing 25 ml of MB solutions with different initial concentrations (0, 5, 6, 10, 14, 20, 25, 40 mg/l) and a 0.5 g of adsorbent added to each solution. These MB solutions were kept under a stirring speed of 450 rpm for 48 h, to ensure that sorption equilibrium was reached. Then the supernatants were fitted and centrifuged before the measurement of its absorbance. The absorbance was measured using a UV–Vis spectrophotometer (SpectroFlex6100) by monitoring the absorbance changes at wavelength of maximum absorbance (663 nm). The MB concentrations were estimated using a calibration curve obtained by plotting the absorbance against the concentration of the MB solution. The amount of dye adsorbed per unit weight of sample (sand or clay) at equilibrium, q_e (mg g^{-1}) was calculated as follow:

$$q_e = \frac{(C_0 - C_e)V}{m} \tag{1}$$

where C_0 and C_e are the initial concentration and liquid-phase concentrations of dye solution at equilibrium (mg L^{-1}) respectively, V is the dye volume (L) and m is the mass of the sample (g). The equilibrium isotherms are important in the description of adsorbate interaction with adsorbent. Several mathematical model of the equilibrium adsorption were developed to predict adsorption parameters and to provide an insight into the adsorption behavior for different adsorbent system. In this study, two important isotherms models are selected, the Langmuir (Langmuir, 1918) and Freundlich (Freundlich, 1906). The non linear form of these models is given as follow:

Freundlich model:

$$q_e = k_F(C_e)^{1/n} \tag{2}$$

Langmuir model:

$$q_e = \frac{q_m b C_e}{1 + bC_e} \tag{3}$$

k_F: Freundlich isotherm constant [(mg g^{-1})(L mg^{-1})$(1 - n/n)$]; n: Freundlich exponent; q_m: Langmuir adsorption capacity (mg g^{-1}); b: Langmuir isotherm constant (L mg^{-1}).

2.2.2. Sorption kinetics

For the sorption kinetics experiments, vials containing 1 g of sample and 20 ml of MB solutions with 150 mg L^{-1} initial concentration were shaken at 450 rpm for 90 min. At the end of the predetermined time interval, the vials were filtered then centrifuged at 2500 tr/min. The supernatant solution was analyzed using UV–Vis spectrophotometer (SpectroFlex6100) to

Table 1 Saturation condition, soil structure, MB initial concentration, flow rate, bed length and dispersion coefficient for column experiments. C_0 is the MB inlet concentration, υ is the flow rate, H is the bed length and D_L is the hydrodynamic dispersion coefficient.

	Exp A	Exp B	Exp C	Exp D	Exp E	Exp F	Exp G	Exp H
Saturation condition	Saturated	Saturated	Saturated	Saturated	Saturated	**Unsaturated** (S = 14.25%)	Unsaturated (S = 72.45%)	Unsaturated (S = 72.45%)
Composition	Homogeneous sand	Homogeneous sand	Homogeneous sand	Homogeneous sand	Homogeneous sand	Homogeneous sand	Homogeneous sand	**Heterogeneous layered medium**
C_0 (mg L^{-1})	100	100	100	**50**	**200**	100	**1000**	1000
υ (mL min^{-1})	**4.6**	**8.5**	**3.2**	8.5	8.5	8.5	30	30
H (cm)	10	10	10	10	10	10	**25**	25
D_L (m^2/s)	$204 \cdot 10^{-5}$	$378 \cdot 10^{-5}$	$145 \cdot 10^{-5}$	$378 \cdot 10^{-5}$	$378 \cdot 10^{-5}$	$4.45 \cdot 10^{-5}$	$32 \cdot 10^{-4}$	$1.36 \cdot 10^{-4}$

determine the dye concentration. Each experiment was replicated 3 times to verify the reproducibility of the experience.

The adsorption capacity, q_t (mg g^{-1}) was calculated as:

$$q_t = \frac{C_0 - C_t}{m} V \quad (4)$$

where q_t is the dye concentration on adsorbent at time t (mg g^{-1}), C_0 and C_t are the concentrations of the MB solution before and after adsorption, respectively (mg L^{-1}), V is the volume of MB solution and m is the mass of dry sample (g). The modeling of adsorption kinetics is necessary for the prediction of the MB removal from the aqueous solution to solid surface and to describe the adsorption in solid–liquid systems. Much adsorption kinetics model has been proposed by several researchers (Kumar and Sivanesan, 2006) to supervise the mechanism of adsorption process and to test the experimental data. The pseudo-first–order kinetics also known as the Lagergren, the pseudo-second–order kinetics, the Elovich and the intraparticle diffusion model were used to determine the constant rate of the dye removal from the solution to the sample (Lagergren, 1898; Elovich, 1959). There are many types of the pseudo-second order kinetic equation but in the dye adsorption process, the types 1 and 2 describe more the fitting of kinetic models (Wawrzkiewicz and Hubicki, 2009). Thus, the study of pseudo- second order kinetic is limited to types 1 and 2 in this work. The non linear form of pseudo-second-order equation is given as:

$$\frac{t}{q_t} = \frac{1}{k_2 q_e^2} + \frac{t}{q_e} \quad (5)$$

where qt (mL/kg) is the amount of MB adsorbed at time t (min); k_2 (kg mL^{-1} min^{-1}) is the rate constant of pseudo second-order adsorption; and q_e (mL/kg) is the amount of MB adsorbed per mass of the material at equilibrium.

2.3. Column experiment

A series of fixed bed column experiments have been performed to determine the MB behavior in saturated and unsaturated soil and to study the effect of heterogeneity on MB transfer. The column used in the experiments was made with glass and has a dimension of 3.5 cm in diameter and 25 cm in length. The fixed bed column used is 10 cm. The column experiments were conducted at constant flow rate (Q = 8.5 mL min^{-1}) and the initial MB concentration (C_0 = 100 mg L^{-1}) under saturated or unsaturated flow conditions. Then the MB was eluted from the column by rainwater flushing. During the experiment, the effluent samples were collected at the column outlet and measured for MB concentration immediately after sampling. The MB concentrations in the column effluents were determined using UV–Vis spectrophotometer. The MB breakthrough curves (BTC) were obtained by plotting relative concentrations (C/C_0) versus time (t).

3. Breakthrough curves modeling

The breakthrough curves modeling allows the evaluation of fixed bed column performance. In this study two approaches have been investigated for data fitting of MB breakthrough curves on and clay materials. These models include Thomas and convection dispersion equations.

3.1. Thomas model

The Thomas model assumes that a Langmuir isotherm and second order kinetic fitted well the experimental data. It was also assumed that adsorption is limited by mass transfer and no axial dispersion is derived with adsorption. It allows the calculation of the adsorption rate constant. The equation of Thomas model can be described as:

$$\frac{C_t}{C_0} = \frac{1}{1 + \exp\left((q_0 m - C_0 \vartheta t)\frac{k_{th}}{\vartheta}\right)} \quad (6)$$

where k_{th} is Thomas rate constant (mL min^{-1} mg^{-1}), q_0 is equilibrium adsorption capacity (mg g^{-1}), m is the mass of the adsorbent, C_0 and C_t are the MB concentration in the influent and at time t (mg L^{-1}) and υ is the flow rate (mL min^{-1}).

The Thomas rate constant (k_{th}), adsorption capacity (q_0), and the correlation coefficient (R^2) in different operations conditions were calculated by non linear regression analysis (see Table 2). In this table, the k_{th} values decrease with the increase in influent MB concentration. The values of k_{th} decreased due to the high driving force for adsorption caused by the concentration gradient. The maximum adsorption capacity q_0 increases with the increase in initial MB concentration. The correlation coefficient values ranging from 0.875 to 0.988 indicate a good agreement between the experimental data and the fitted data generated using Thomas model. It is clear also from Table 3 that in the heterogeneous soil(Exp H), the equilibrium adsorption capacity (q_0) found to be the higher value compared to homogeneous soil. This is due to the soil heterogeneity and the presence of clay layer with high cationic exchange capacity with MB in the bed column.

Table 2 Thomas model parameters at different flow rate, inlet MB concentration, saturation condition and soil heterogeneity.

	k_{th} (ml min^{-1} mg^{-1})*10^{-4}	q_0 (mg g^{-1})*10^3	R^2
Exp A	5.54	0.59	0.972
Exp B	4.01	0.56	0.988
Exp C	2.58	0.50	0.969
Exp D	4.03	0.74	0.918
Exp E	1.82	1.13	0.972
Exp F	4.01	0.56	0.986
Exp G	0.0553	2.74	0.9535
Exp H	0.075	32.17	0.877

Table 3 Soil hydraulic and solute transport parameters θ_s, θ_r, K_S are the saturated water content, the residual water content and the hydraulic conductivity, respectively, α and n are the van Genuchten parameters (van Genuchten, 1980) and ρ_b is the bulk density.

Parameters	Sand	Clay
θ_s	0.31	0.508
θ_r	0.06	0.258
K_S (ms^{-1})	$225 \cdot 10^{-5}$	$336 \cdot 10^{-7}$
α (cm^{-1})	0.0259	0.044
n	2.8	2.002
ρ_b (g cm^{-3})	1.34	1.45

3.2. Advection–dispersion model

A general transport and adsorption model for a porous medium was used to predict dynamic adsorption breakthrough. This model is based on convection dispersion equation (Eq. (7)) for two dimensional flows through a porous bed.

$$\frac{\partial(\theta C)}{\partial t}+\frac{\partial}{\partial t}(\rho_b C_p)+\nabla(-\theta D_L \nabla C+UC)=\sum R+\sum S \quad (7)$$

where C and C_p are the adsorbate concentration in the liquid and solid phases, respectively (kg m^{-3}), ρ_b is the bulk density (kg m^{-3}), θ is the bed water content, k_p is the adsorption rate (m^3 kg^{-1}), U is the Darcy velocity (m s^{-1}), R and S are the reaction and D_L is the hydrodynamic dispersion tensor.

The rate of accumulation in the solid phase term $\left(\frac{\partial C_p}{\partial t}\right)$ was accounted for the following equation:

$$\frac{\partial C_p}{\partial t}=\alpha(K_L C(q_m-C_p)-C_p) \quad (8)$$

α is the rate constant (s^{-1}), q_m is the maximum Langmuir adsorption parameter, Cp is the adsorbent capacity (kg m^{-3}) and K_L is the Langmuir adsorption parameter (m^3 kg^{-1}).

Severe incorporation of Richard equation (Eq. (9)) is to describe the Darcy flow through porous media was coupled with advection dispersion-equation. This coupling is through Darcy velocity equation (Eq. (10)). The Richard equation is expressed as follows:

$$(C+S_e S)\frac{\partial H_p}{\partial t}+\nabla(-K\nabla(H_p+D))=Q_m \quad (9)$$

$$u=K_s k_r \nabla(H_p+D) \quad (10)$$

where H_p is the pressure head (m), C is the specific moisture capacity, S_e represents the effective saturation, S is the storage coefficient, K is the hydraulic conductivity, k_r is the relative permeability, D represents the elevation (m), and Q_m is the fluid source or sink. The unsaturated soil properties were described using the van Genuchten model.

$$K(\theta)=K_S S_e^2[1-(1-S_e)^{1/m}]^m \quad (11)$$

where m is the van Genuchten parameter and K_S denotes the hydraulic permeability.

The initial and boundary condition for two dimensional problems used for solving this model are:

$$C(z,0)=0$$

$$C(L,t)=C_0$$

$$\frac{\partial C}{\partial z}(0,t)=0$$

$$C_p(z,0)=0$$

4. Results and discussion

4.1. Samples characterizations

The results of X-ray spectroscopy show the presence of smectite clay. The smectite clay is characterized by its cationic exchange capacity in the interlayer spaces. The value of this CEC is found to be equal to 90 meq/100 g of clay.

The X-ray diffraction pattern (Fig. 1a) had three significant reflections at 15.6°A, 3.34°A and 1.45°A. The two reflection distances of 3.31°A and 1.45°A indicated the presence of silice and that the clay is a dioctahedral smectite, respectively. The isomorphic cationic exchange in the interlayer spaces caused by the substitution of Al^{+3} by Mg^{+2} provides a deficit in charge. This negative charge is obviously compensated by an equal number of cations. Also, this mineral clay has the ability to swell in the presence of water. So the smectite clay fixes the water by adsorption to its surface and increases in volume by swelling, however this swelling decreases with the increase in layer charges. The reflection distance of 15.6°A proves that the clay is calcic clay. The particle size analysis of sand and clay samples shows that the fifty percent passing particle size (d_{50}) was calculated as 317 μm and 11.69 μm based on sieve sizing for sand and clay, respectively (Fig. 1b).

4.2. Adsorption models

The sorption behavior of MB in clay and sand was tested using non linear fitting. The good fitting of the model with experimental data is represented by a high value of correlation coefficient. For the clay, the Freundlich model provides a better fit in the MB adsorption isotherm (Fig. 2a). The Freundlich isotherms model predicts multilayer adsorption and describes equilibrium on heterogeneous surfaces. The applicability of Langmuir isotherm for sand material implies that monolayer adsorption exist under the experimental conditions. The prediction of kinetics adsorption is needed to evaluate the adsorption efficiency using two models. The pseudo first order

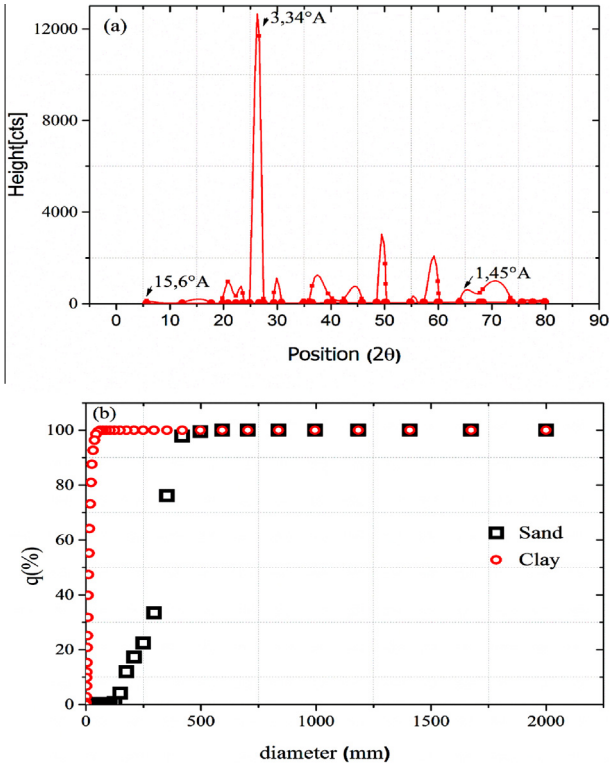

Figure 1 (a) XRD diagram of smectite clay and (b) particle size distribution of Sand and clay.

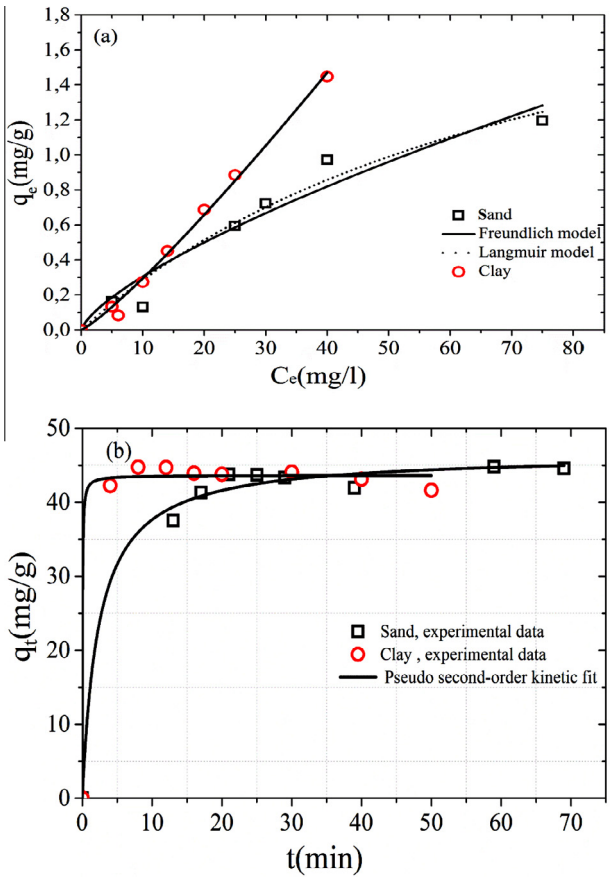

Figure 2 (a) Langmuir and Freundlich adsorption isotherms of MB and (b) pseudo second-order kinetic adsorption of MB.

Table 4 Isotherm and kinetic adsorption modeling parameters.

Models		Freundlich	Langmuir	Pseudo-second order kinetic
Materials	Sand	k_F = 0.0639 n = 1.36 R^2 = 0.845	b = 0.0117 q_{max} = 3.117 **R^2 = 0.874**	q_e = 46.49 k_2 = 0.00916 **R^2 = 0.9912**
	Clay	k_F = 0.0136 n = 0.826 **R^2 = 0.995**	b = 0.00224 q_{max} = 13.72 R^2 = 0.97893	q_e = 43.65 k_2 = 0.711 **R^2 = 0.994**

equation represented very shabbily the kinetic data of MB in sand and clay. The best regression of experimental data for both sand and clay is using the type 1 of pseudo second order kinetic equation (Fig. 2b). The parameters of isotherms and kinetic adsorption models are presented in Table 4.

4.3. Column experiments

4.3.1. Effect of flow rate on BTC

The effect of flow rate on MB adsorption has been studied at three flow rates (3.2, 4.6 and 8.5 mL min^{-1}). The initial MB concentration was 100 mg L^{-1} and the bed height was 10 cm (Exp A, Exp B and Exp C). Breakthrough curves obtained on MB adsorption by sand at three flow rates are presented in figure (Fig. 3a). It is clear from this figure that the breakthrough time decreases with the increasing flow rate. As the

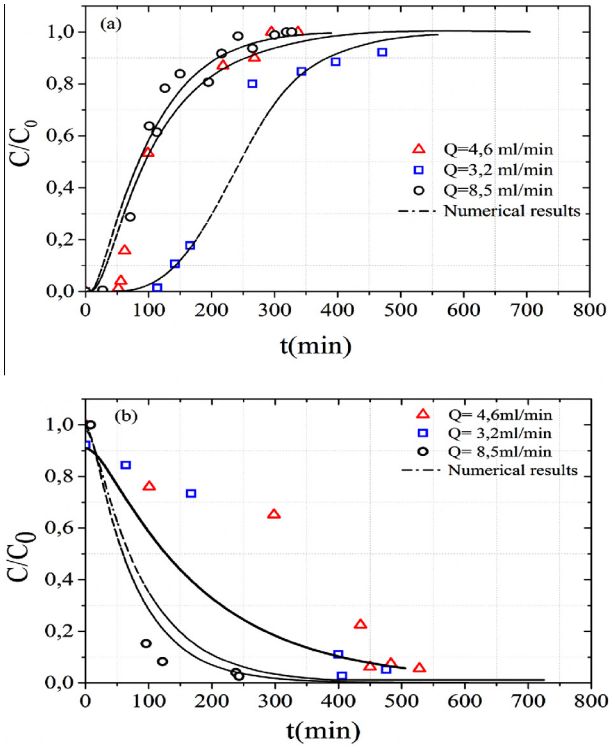

Figure 3 Effect of flow rate on the (a) MB adsorption and (b) MB desorption.

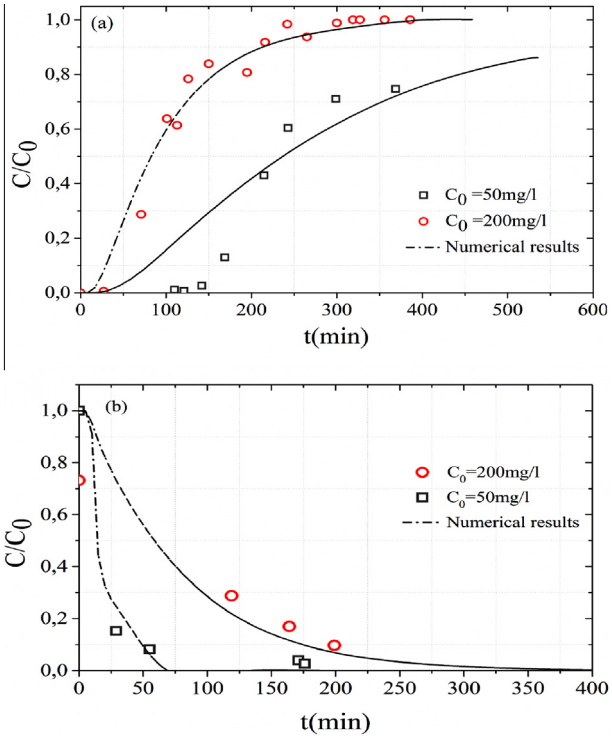

Figure 4 Effect of initial concentrations on the (a) MB adsorption and (b) MB desorption.

flow rate increased from 3.2 to 8.5 mL min^{-1}, the breakthrough time decreased from 114 to 27 min. This increase of the flow rate reduced the contacting time of the MB with the adsorbent in the column and limited by the diffusion of the MB into the pores of the materials. This insufficient residence time of the MB in column reduces the adsorption capacity (Uddin et al., 2009).

4.3.2. Effect of initial MB concentration on BTC

The effects of initial MB concentration have been investigated at 50 mg L^{-1} and 200 mg L^{-1} (Exp D and Exp E). The flow rate was fixed at 8.5 mL min^{-1} and the bed height was 10 cm. Breakthrough curves obtained on MB adsorption by sand at two initial concentrations are presented in Fig. 4. It was obvious that as the influent concentration increased the breakthrough curves became sharper and the breakthrough time decreased (Zhang et al., 2011). They indicate that with an increase in the initial MB concentration, the adsorption sites were occupied much faster and MB solution took less time to reach the saturation time.

4.3.3. Effect of initial saturation condition of soil on BTC

The saturation condition of soil affects the BTC (Fig. 5a). In both experiments (Exp B and Exp F), the bed length is 10 cm, the initial concentration is 100 mg L^{-1} and the flow rate is 8.5 mL min^{-1}. In the unsaturated media, the pores are partially filled with water. The MB transport in unsaturated medium causes an increase in the MB dispersion (spreading of BTC) and a faster output of effluent from the column. This fast transport reduces the breakthrough time and increases effluent tailing. Fig. 5(c) represents the spatial evolution of adsorbed concentration in solid phase. At the beginning (after 50 min of MB injection) and in the middle (after 150 min of MB injection) of experience (Exp F), the retention (adsorption) rate in unsaturated soil is higher than in saturated soil. The increase of moisture content in porous media decreases the amount of particles adsorbed onto substances, the adsorption capacity and the kinetic rate (Fig. 5c). This decrease is in agreement with the second order kinetic model hypothesis that the adsorption only depends on the surface sites (Liu, 2008). In addition, the water molecule has a diameter lower than the MB molecule, which makes it more difficult for MB solution to penetrate through the pore space of the medium in unsaturated medium. The methylene blue solution wets the dry grain and simultaneously adsorbed on the external surface of grain. This coupled action between wetting and adsorption phenomena causes a strong fixation of methylene blue particles on the solid phase which prevents their release during leaching. This may be the reason that the methylene blue desorption in the unsaturated medium is slower than the saturated soil (Fig. 5b).

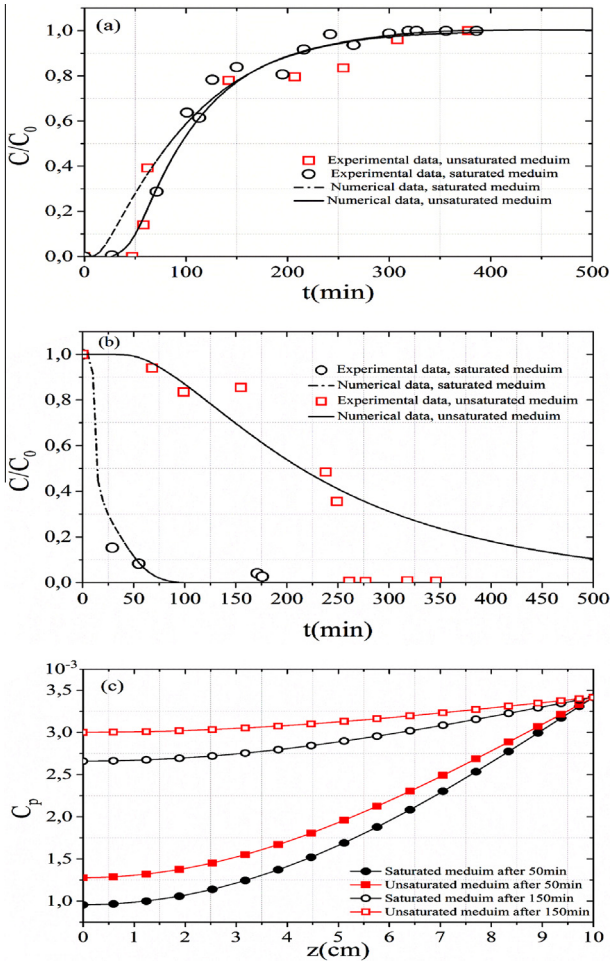

Figure 5 Effects of saturation condition on the (a) MB adsorption, (b) MB desorption and (c) adsorbed concentration in solid phase along with fixed bed column.

4.3.4. Effect of the soil heterogeneity on BTC

Fig. 6(a) shows the influence of soil heterogeneity in BTC. The fixed bed length is 25 cm and the MB inlet concentration is

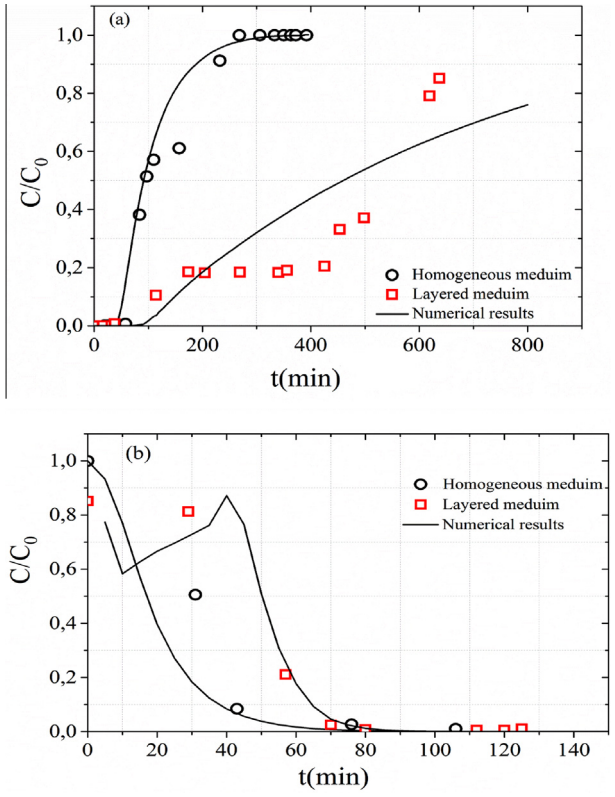

Figure 6 Effects of soil heterogeneity on the (a) MB adsorption and (b) MB desorption.

Table 5 Error analysis of fitting models of the MB breakthrough curves.

Model	Error (%)							
	Exp A	Exp B	Exp C	Exp D	Exp E	Exp F	Exp G	Exp H
Thomas model	33.36	14.33	27.42	49.36	17.54	20.23	29.5	69.41
Advection–dispersion model	32.19	12.44	17.11	47.14	12.9	14.98	17.12	44.75

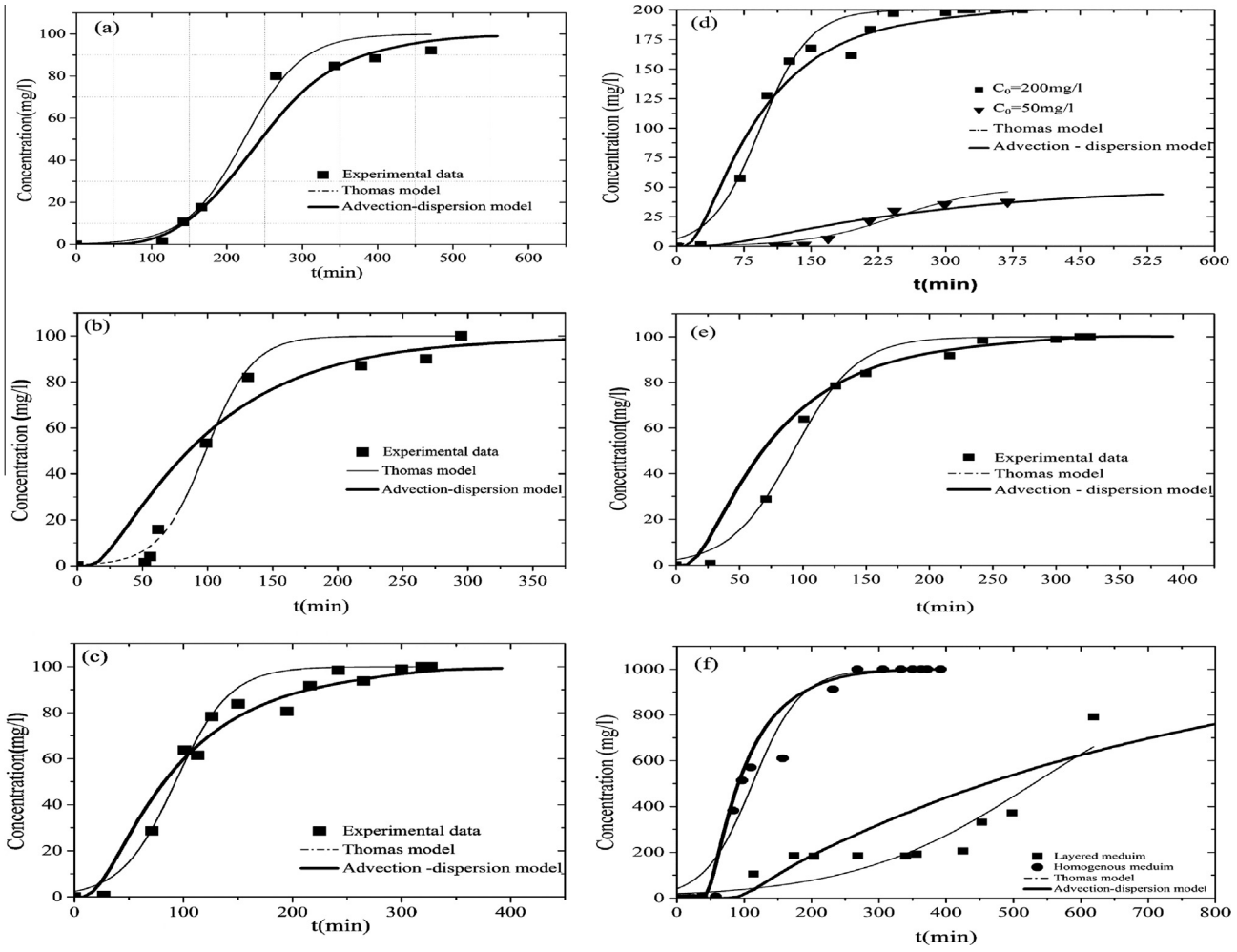

Figure 7 Experimental and predicted breakthrough curves for MB adsorption. (a) Exp A, (b) Exp C, (c) Exp B, (d) Exp D and Exp E, (e) Exp F and (f) Exp G and Exp H.

1000 mg L^{-1} and the flow rate of $Q = 8.5$ mL min^{-1}. The difference in the MB behavior between its infiltration into a homogeneous and heterogeneous unsaturated porous medium is clear. The heterogeneous soil consists of two layers. The first part comprises a layer of sand (20 cm, in thick) placed above a layer of clay (5 cm, in thick) to create a capillary barrier at the interface between the sand and the clay material.

The peaks of the MB breakthrough curves for heterogeneous medium is of order 0.88 ($C/C_0 = 0.88$) while that of homogeneous medium is higher (Fig. 6a). In the unsaturated heterogeneous layered medium, the hydrodynamic proprieties of the two materials caused the prevention of water and flow through the interface and forced the water accumulation at the interface until water pressure head is enough to permit it to penetrate (Li et al., 2013). The increase in water pressure head associated with water accumulation at the interface of two materials shows a capillary barrier effect. In this interface the retention is more important (Prédélus et al., 2015). After 100 min, the gradient of MB adsorbed concentration in $z = 5$ cm (interface between sand and clay materials) is more important compared to homogeneous medium. This increase of retention capacity in this interface results from an increase in the water content and the decrease in pore water velocity improves the MB solution entrapment (Torkzaban et al., 2008). Indeed, the decrease in pore water velocity is accompanied with a decrease in kinetic adsorption rate at the interface.

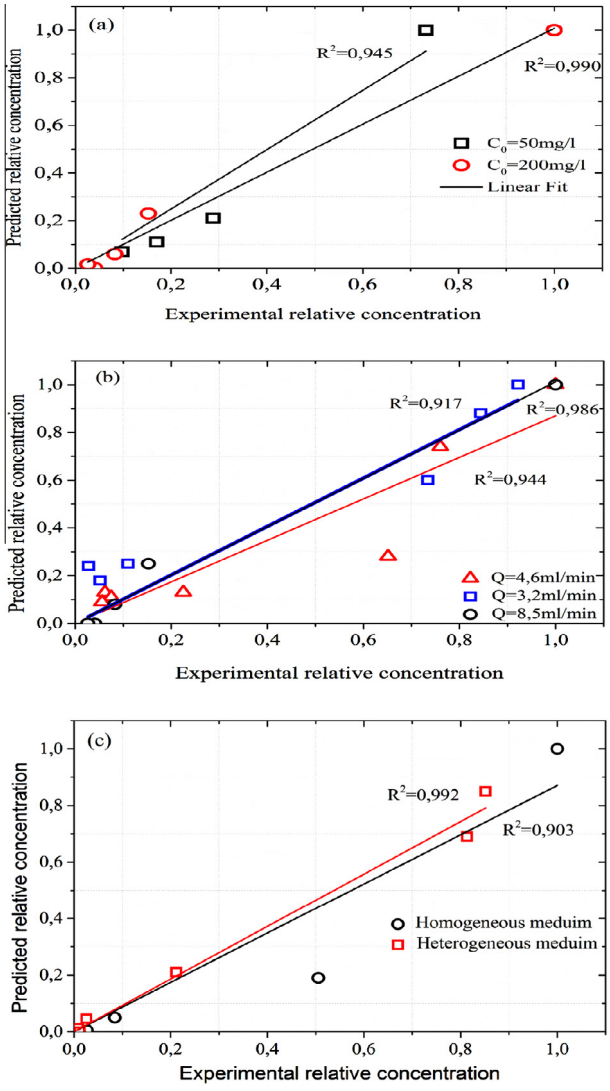

Figure 8 Predicted data from advection dispersion model against experimental data of MB desorption experiments at (a) different flow rate, (b) different initial concentration and (c) homogeneous and heterogeneous porous media.

4.4. Advection–dispersion model effectiveness

The experimental MB adsorption data are fitted using the proposed models. The average error (E (%)) of used models which are reported in Table 4 were calculated using

$$E(\%) = \frac{100}{N}\sum_{i=1}^{N}\left|\frac{(C/C_0)_{\text{experimental}} - (C/C_0)_{\text{predicted}}}{(C/C_0)_{\text{predicted}}}\right| \quad (12)$$

where N is the number of experimental points.

In all experiments for the advection–dispersion model the fitting errors are lower than those of Thomas model. Consequently, it might be provided that the Thomas model can fail for breakthrough curve data correlation because this model considers an adsorption–desorption process with negligible axial dispersion (see Table 5).

The contrast between the errors of Thomas model and those of advection dispersion model becomes huge in the unsaturated heterogeneous porous media. This confirms that the advection dispersion model makes a good reproduction of mechanisms of transfer in porous media and seems to be a useful tool to better understanding the physical processes and the effect of capillary barrier of MB transport in unsaturated heterogeneous soil (Fig. 7).

4.5. Desorption studies

The study of MB release from soil is important for understanding MB movement in the soil. Desorption is followed immediately after MB adsorption. Column desorption experiments were performed using rain water. The predicted relative concentration of desorption experiments were calculated using advection dispersion model. The determination coefficient of this model ranging from 0.903 to 0.99 (Fig. 8a–c) indicated that advection–dispersion model provided the best description of MB desorption behavior in soil.

5. Conclusion

From batch and fixed bed experimental data of MB adsorption and transport in soils and fixed bed column modeling, the following conclusions are taken:

- The adsorption isotherm is described using Langmuir model for sand and Freundlich model for clay and sand/-clay mixture.
- The adsorption kinetic is described using pseudo second order model for both materials (sand and clay).
- Experimental data revealed that the breakthrough curves depend on flow rate, MB inlet concentration, saturation condition of soil and soil heterogeneity.
- The decrease in moisture content in porous media increases the amount of particles adsorbed onto substances, the adsorption capacity and the kinetic rate.
- The increase in water pressure head associated with water accumulation at the interface of two materials increases the retention capacity in this interface and decreases the pore water velocity.
- The decrease in pore water velocity is accompanied with a decrease in kinetic adsorption rate at the interface of sand and clay materials.
- In heterogeneous medium, the equilibrium adsorption capacity (q_0) of Thomas model has the higher value compared to homogeneous medium.
- The comparative analysis between both models proves that advection–dispersion model is the suitable one to describe the adsorption and transportation of MB in saturated and unsaturated soil.
- The comparison of the experimental breakthroughs with breakthrough simulations in desorption experiments shows that the advection–dispersion model provided the best description of MB desorption behavior in soil.
- The methylene blue desorption in the unsaturated medium is slower than the saturated soil.

Acknowledgements

The authors would like to thank the personnel (H. Majdoub, S. Dhawadi and H. Ben Jannet; Faculty of Science, Monastir)

that helped make this work a success. As well, the authors would like to thank A. Baffoun and A. Moussa for their assistance in the analysis by spectrophotometer.

References

AFNOR, NF X 31-130 soil quality, 1999. Chemical methods, Determination of Cation Exchange Capacity (CEC) and Cation Extraction. AFNOR, Paris.

Auta, M., Hameed, B.H., 2014. Chitosan–clay composite as highly effective and low-cost adsorbent for batch and fixed-bed adsorption of methylene blue. Chem. Eng. J. 237, 352–361.

Bukallah, S.B., Rauf, M.A., AlAli, S.S., 2007. Removal of methylene blue from aqueous solution by adsorption on sand. Dyes Pigm. 74 (1), 85–87.

Dotto, G.L., dos Santos, J.N., Rosa, R., Pinto, L.A.A., Pavan, F.A., Lima, E.C., 2015. Fixed bed adsorption of methylene blue by ultrasonic surface modified chitin supported on sand. Chem. Eng. Res. Des. 100, 302–310.

Elovich, S.J., Schulman, J.H. (Eds.), 1959. Proceedings of the Second International Congress on Surface Activity, vol. 11. Academic Press Inc., New York, p. 253.

Foo, K.Y., Hameed, B.H., 2011. Preparation of activated carbon from date stones by microwave induced chemical activation: application for methylene blue adsorption. Chem. Eng. J. 170 (1), 338–341.

Freundlich, H.M.F., 1906. Over the adsorption in solution. J. Phys. Chem. 57 (385), e470.

Guo, J.Z., Li, B., Liu, L., Lv, K., 2014. Removal of methylene blue from aqueous solutions by chemically modified bamboo. Chemosphere 111, 225–231.

Hamdaoui, O., 2006. Dynamic sorption of methylene blue by cedar sawdust and crushed brick in fixed bed columns. J. Hazard. Mater. B138, 293–303.

Han, R., Wang, Y., Zou, W., Wang, Y., Shi, J., 2007. Comparison of linear and nonlinear analysis in estimating the Thomas model parameters for methylene blue adsorption onto natural zeolite in fixed-bed column. J. Hazard. Mater. 145 (1), 331–335.

Han, R., Wang, Y., Zhao, X., Wang, Y., Xie, F., Cheng, J., Tang, M., 2009. Adsorption of methylene blue by phoenix tree leaf powder in a fixed-bed column: experiments and prediction of breakthrough curves. Desalination 245 (1), 284–297.

Kumar, K.V., Sivanesan, S., 2006. Pseudo second order kinetic models for safranin onto rice husk: comparison of linear and non-linear regression analysis. Process Biochem. 41 (5), 1198–1202.

Lagergren, S., 1898. About the theory of so-called adsorption of soluble substances, K. Sven, Vetenskapsakad. Handl. Band. 24, 1–39.

Langmuir, I., 1918. Adsorption of gases on plain surfaces of glass mica platinum. J. Am. Chem. Soc. 40, 1361–1403.

Li, Z., Chang, P.H., Jiang, W.T., Jean, J.S., Hong, H., 2011. Mechanism of methylene blue removal from water by swelling clays. Chem. Eng. J. 168 (3), 1193–1200.

Li, J.H., Du, L., Chen, R., Zhang, L.M., 2013. Numerical investigation of the performance of covers with capillary barrier effects in South China. Comput. Geotech. 48, 304–315.

Liu, Y., 2008. New insights into pseudo-second order kinetic equation for adsorption. Colloids Surf. A 320, 275–278.

Liu, Y., Wang, J., Zheng, Y., Wang, A., 2012. Adsorption of methylene blue by kapok fiber treated by sodium chlorite optimized with response surface methodology. Chem. Eng. J. 184, 248–255.

Makrigianni, V., Giannakas, A., Deligiannakis, Y., Konstantinou, I., 2015. Adsorption of phenol and methylene blue from aqueous solutions by 2 pyrolytic tire char: equilibrium and kinetic studies. J. Environ. Chem. Eng. 3 (1), 574–582.

Mitrogiannis, D., Markou, G., Çelekli, A., Bozkurt, H., 2015. Biosorption of methylene blue onto Arthrospira platensis biomass: kinetic, equilibrium and thermodynamic studies. J. Environ. Chem. Eng 3 (2), 670–680.

Prédélus, D., Coutinho, A.P., Lassabatere, L., Bien, L.B., Winiarski, T., Angulo-Jaramillo, R., 2015. Combined effect of capillary barrier and layered slope on water, solute and nanoparticle transfer in an unsaturated soil at lysimeter scale. J. Contam. Hydrol. 181, 69–81.

Rauf, M.A., Bukallah, S.B., Hamour, F.A., Nasir, A.S., 2008. Adsorption of dyes from aqueous solutions onto sand and their kinetic behavior. Chem. Eng. J. 137 (2), 238–243.

Reza, R.A., Ahmaruzzaman, M., 2015. Comparative study of waste derived adsorbents for sequestering methylene blue 3 from aquatic environment. J. Environ. Chem. Eng. 3 (1), 395–404.

Sadasivam, B.Y., Reddy, K.R., 2015. Adsorption and transport of methane in landfill cover soil amended with waste-wood biochars. J. Environ. Manage. 158, 11–23.

Şahin, Ö., Kaya, M., Saka, C., 2015. Plasma-surface modification on bentonite clay to improve the performance of adsorption of methylene blue. Appl. Clay Sci. 116, 46–53.

Thomas, H.C., 1944. Heterogeneous ion exchange in a flowing system. J. Am. Chem. Soc. 66 (10), 1664–1666.

Tian, Y., Gao, B., Ziegler, K.J., 2011. High mobility of SDBS dispersed single walled carbon nanotubes in saturated and unsaturated porous media. J. Hazard. Mater. 186 (2–3), 1766–1772.

Torkzaban, S., Bradford, S.A., van Genuchten, M.T., Walker, S.L., 2008. Colloid transport in unsaturated porous media: the role of water content and ionic strength on particle straining. J. Contam. Hydrol. 96 (1), 113–127.

Uddin, M.T., Rukanuzzaman, M., Khan, M.M.R., Islam, M.A., 2009. Adsorption of methylene blue from aqueous solution by jackfruit (*Artocarpus heteropyllus*) leaf powder: a fixed-bed column study. J. Environ. Manage. 90 (11), 3443–3450.

van Genuchten, M.T., 1980. A Closed-form equation for predicting the hydraulic conductivity of unsaturated soils. Soil Sci. Soc. Am. J. 44 (5), 892–898.

Wang, S., Li, H., Xie, S., Liu, S., Xu, L., 2006. Physical and chemical regeneration of zeolitic adsorbents for dye removal in wastewater treatment. Chemosphere 65 (1), 82–87.

Wang, Y., Wang, W., Wang, A., 2013. Efficient adsorption of methylene blue on an alginate-based nanocomposite hydrogel enhanced by organo-illite/smectite clay. Chem. Eng. J. 228, 132–139.

Wawrzkiewicz, M., Hubicki, Z., 2009. Kinetic studies of dyes sorption from aqueous solutions onto the strongly basic anion-exchanger Lewatit MonoPlus M-600. Chem. Eng. J. 150 (2), 509–515.

Winiarski, T., Lassabatere, L., Angulo-Jaramillo, R., Goutaland, D., 2013. Characterization of the heterogeneous flow and pollutant transfer in the unsaturated zone in the fluvio-glacial deposit. Procedia Environ. Sci. 19, 955–964.

Xing, Y., Liu, D., Zhang, L.P., 2010. Enhanced sorption of methylene blue by EDTAD modified sugarcane bagasse and photocatalytic regeneration of the sorbent. Desalination 259 (1), 187–191.

Yang, J., Qiu, K., 2010. Preparation of activated carbons from walnut shells via vacuum chemical activation and their application for methylene blue removal. Chem. Eng. J. 165, 209–217.

Zhang, W., Dong, L., Yan, H., Li, H., Jiang, Z., Kan, X., Cheng, R., 2011. Removal of methylene blue from aqueous solutions by straw based adsorbent in a fixed-bed column. Chem. Eng. J. 173, 429–436.